ELSEVIER

Science and Technology of Advanced Materials 6 (2005) 689–703

SCIENCE AND TECHNOLOGY OF ADVANCED MATERIALS

www.elsevier.com/locate/stam

Review

Various aspects of $LiNiO_2$ chemistry: A review

P. Kalyani, N. Kalaiselvi*

Electrochemical Energy Systems Division, Central Electrochemical Research Institute, Karaikudi 630 006, India

Received 29 March 2005; revised 2 June 2005; accepted 4 June 2005
Available online 6 September 2005

Abstract

Despite the appearance of ever first report on the synthesis of $LiNiO_2$ in 1954, active research to identify and evaluate its suitability as an electrode material in rechargeable lithium batteries started only in late 80's. Following this, numerous articles discussed the synthesis, electrochemical behavior and the problems associated with the compound. In this connection, the present communication reviews certain important experimental results obtained by different research groups on various aspects of $LiNiO_2$, in order to understand the significance of $LiNiO_2$ as a potential cathode material for rechargeable lithium batteries. Also selected type of methodologies adopted to synthesize the title compound have also been discussed to substantiate the dependence of electrochemical behavior of $LiNiO_2$ on the method of synthesis and reaction conditions. The subject has been discussed at length and may provide useful information on the properties of $LiNiO_2$ and may enable the fabrication of tailor made nickel-based electrode materials for 'next generation' lithium or lithium-ion batteries along with the highlights of doped and coated derivatives of $LiNiO_2$.

Keywords: $LiNiO_2$; Lithium nickelate; Electrochemistry; Vibrational spectroscopy; Electronic structure

Contents

* Corresponding author.
E-mail address: kalakanth2@yahoo.com (N. Kalaiselvi).

1468-6996/$ - see front matter © 2005 Elsevier Ltd. All rights reserved.
doi:10.1016/j.stam.2005.06.001

1. Introduction

Nickel compounds find application as electrode materials in battery systems, for instance, in the form of NiO(OH) in Ni–Cd and Ni–MH batteries. In rechargeable lithium batteries, nickel is employed in the form of oxide in which lithium ions are intercalated (inserted) in to its crystal structure at about 4 V to form layered nickel oxide viz., $LiNiO_2$ [1–3]. For several years nickel oxide is very much known for its electro chromicity [4], where protons serve as the guest, intercalating into the nickel oxide host structure at a lower voltage. Possibly, this compound might have been the origin of $LiNiO_2$, wherein the Li^+ ion exchange occurs at a voltage as high as 4 V. Though the origin of $LiNiO_2$ dates back to early 1950's [5], $LiNiO_2$ has been accepted as one of the attractive cathode materials for rechargeable lithium batteries just two decades back only [6]. Consequently, nickel based oxide cathodes have advanced technological applications as electrode materials and hence an in-depth understanding of various aspects of $LiNiO_2$ assumes paramount significance.

It is well documented that the electrochemical performance of any battery system relies particularly upon the characteristics of the cathode material that is being used [7]. Despite the fact that materials based on sulfides and oxides are known to be viable cathodes, oxides are only considered to be the preferred materials that can be synthesized and employed as cathode materials in an extensive range of lithium battery applications. More commonly, transition metal oxides having spinel structure like that of $LiMn_2O_4$ and with layered structure having the general formula, $LiMO_2$ (M = Co and Ni) [8,9] are being widely employed as cathodes in commercial lithium batteries. Though $LiCoO_2$ and $LiMn_2O_4$ are bestowed with almost similar electrochemical behavior, only the former is able to enjoy its share in the lithium battery market, in spite of its toxicity and high cost [10]. Notwithstanding the advantages of low cost, abundance and eco-friendliness, the inherent problem of Jahn–Teller effect associated with the unacceptable capacity fade upon cell cycling badly limits the utility of $LiMn_2O_4$ as a promising cathode material and thus could provide only a small room for commercial viability of $LiMn_2O_4$ cells, falling next to $LiCoO_2$. As a consequence, the economic and environmental problems of $LiCoO_2$ and the unavoidable decline in discharge capacity of $LiMn_2O_4$ upon cycling has left the door open to exploit $LiNiO_2$ as the choice of cathode candidate of investigation.

For a decade, there has been much hype over $LiNiO_2$—the nickel analog of $LiCoO_2$ and is inviting global attention as an efficient cathode for lithium batteries. Electrochemical studies using $LiNiO_2$ show that it has an edge over the other cathode materials because of its unprecedented capacity of >160 mA/g, excellent cycle life with negligible capacity fading and a deep discharging capability well below 2 V [11]. In addition, at elevated temperatures, both $LiNiO_2$ and $LiCoO_2$ tend to undergo phase transition from hexagonal to a cubic phase and hexagonal phase is electrochemically active while cubic is not. Interestingly, the phase transition for $LiCoO_2$ is reversible, whereas the phase for $LiNiO_2$ is only partially reversible and slow. Hence, stoichiometric $LiNiO_2$ is difficult to be synthesized. Thus, the only disadvantage of $LiNiO_2$ is that it requires utmost care in the synthesis process else will the resulting $LiNiO_2$ sample suffer from twin intricacies namely, cation mixing and off-stoichiometry. Cation mixing in general leads to a composition of $Li_{1-x}Ni_{1+x}O_2$ with $x \sim 0.02$ and studies with this compound resulted in declined electrochemical performance. These two complications make the compound to gain lesser acceptance as a cathode material in the power front. Furthermore, studies reveal that the electrochemical properties of $LiNiO_2$ cathode are extremely dependent upon the synthesis conditions and hence the optimization of preparation conditions [12] of $LiNiO_2$ is essential in order to minimize the said constraints.

Evidently, it is indisputable that $LiNiO_2$ deserves global attention and investigation, which in turn would lend itself as yet another better candidate for 4-volt lithium batteries.

Extensive research has already been initiated by various research groups on the optimization of synthesis conditions of $LiNiO_2$, crystal chemistry, magnetic, electrochemical and several other important aspects of $LiNiO_2$. Such studies are being carried out with a view to have an insight on the correlation between physical and electrochemical properties of $LiNiO_2$ and to obtain nickel based cathode systems with superior performance for lithium and lithium-ion cells. An elaborate discussion regarding the above subjects reported by various research groups has been consolidated here for better understanding and to envisage the importance of the advanced cathode material, $LiNiO_2$.

Apart from the feasibility studies on native $LiNiO_2$ and $LiCoO_2$ cathodes, efforts are being made especially in the recent years to modify the layered frame work in order to circumvent the capacity and safety related limitations [13]. Such attempts are also mentioned in the present communication in order to have better understanding about the effect of each technique so as to arrive at a practically viable potential cathode for next generation lithium batteries.

1.1. Crystal structure of $LiNiO_2$ from XRD

In the ideal stoichiometric $LiNiO_2$ (see Chart 1 for XRD data. JCPDS # 9-063), the Li^+ and Ni^{3+} cations are supposed to be orderly arranged along the (111) direction of the rock salt cubic lattice leading to a 2D layer structure, isostructural with α-$NaFeO_2$ [14]. Hence, $LiNiO_2$ has a rhombohedral structure with trigonal symmetry (space group: *R-3m*) comprising of two interpenetrating close-packed FCC sub-lattices: one consists of oxygen anions, and the other consists of Li and Ni cations on alternating (111) planes. The individual coordinated octahedral sites are edge-sharing. Ni cations are located in octahedral *3b* (0 0 1/2) sites and oxygen anions are in a cubic close-packing, occupying

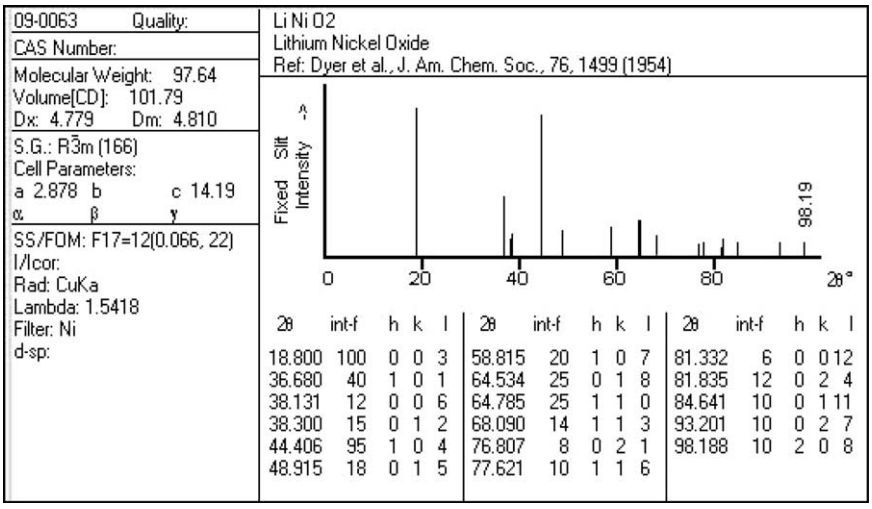

Chart 1. JCPDS data of $LiNiO_2$ (#09-0063) '© JCPDS—International Centre of diffraction Data. All rights reserved' Courtesy: ICDD, publishers of the Powder diffraction file™, 12 Campus Boulevard, Newtown Square, Pennsylvania, USA and Dyer et al., J. Am. chem. Soc., 76, 1499 (1954).

the *6c* (0 0 *z*) sites. Li cations reside at Wyckoff *3a* (0 0 0) sites, represented as $[Li]_{3a}[Ni]_{3b}[O_2]_{6c}$ and the Bravais unit cell contains one formula unit ($Z=1$) [15]. In the rhombohedral crystal structure shown in Fig. 1, the NiO_6 octahedra of trigonal symmetry share their edges to form a triangular Ni-lattice such as depicted at the left side of the figure. The inter-Ni sheet distance (4.73 Å) is much longer than the intra-sheet Ni–Ni distance (2.88 Å).

The structure of $LiNiO_2$ provides the basis of the triangular lattice (TRI) at low temperatures and enables one to intercalate and deintercalate Li^+ reversibly at high temperatures. The cell dimensions of $LiNiO_2$ ($a_h=2.9$ Å and $c_h=14.2$ Å, $c_h/a_h=4.9$ in hexagonal settings) are very much closer to the corresponding values of a cubic cell ($a_h=c_h/23=4.1$ Å), suggesting that the displacement of Ni and Li ions occur easily without any dimensional mismatch compared to that of $LiCoO_2$. This leads to severe structural complexity, which makes the synthesis of stoichiometric and perfect-layer structured $LiNiO_2$ more difficult. In this context, $LiNiO_2$ is best represented as a solid solution denoted by $Li_xNi_{2-x}O_2$ ($0<x<1$) with $LiNiO_2$ ($x=1$) and NiO ($x=0$) as the end members, the JCPDS data of which has been given in Charts 1 and 2, respectively. As x decreases, there exists an increasing amount of Ni^{2+} ions within the Li layers. This reduces the amount of effective lithium ions in the structure thereby increasing the cell

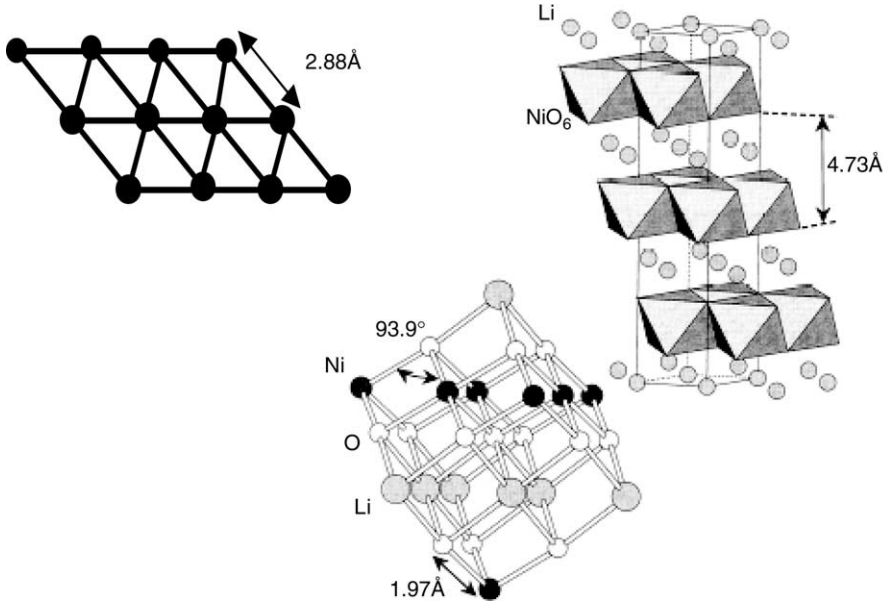

Fig. 1. α-$NaFeO_2$ structure. A hexagonal cell is shown with the solid and dotted lines (right). The Ni–O and Li–O bonds constituting the hexagonal lattice are also shown (middle). The NiO_6 octahedra of trigonal symmetry share their edges to form a triangular Ni lattice such as depicted at the left. [Ref.: M. Takano et al., Mater. Sci. Eng. B63 (1996) 6]

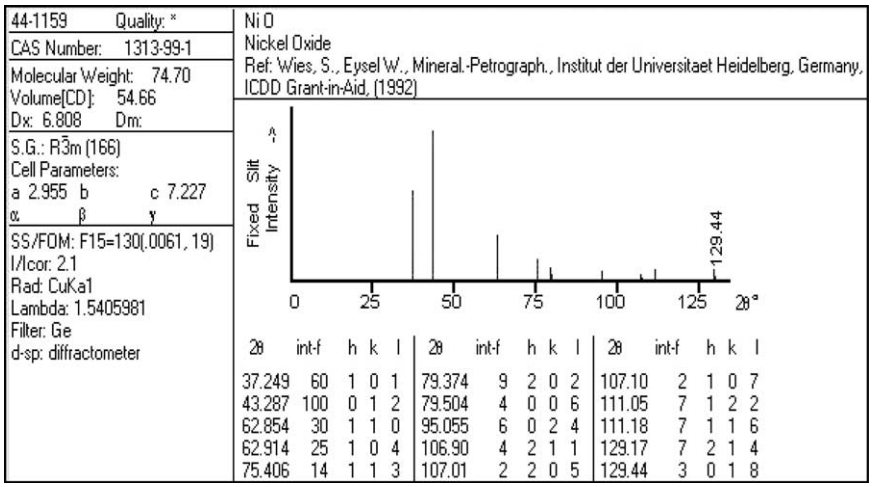

Chart 2. JCPDS data of NiO (#44-1159) '©JCPDS–International Centre for Diffraction Data. All rights reserved'. Courtesy: ICDD [Grant-in-aid (1992)], publishers of the Power Diffraction File™, 12 Campus Boulevard, Newtown Square, Pennsylvania, USA and S. Wies, W. Eysel, Mineral—Petrograph, Institut der Universitaet Heidelberg, Germany.

polarization, which affects ultimately the electrochemical capacity and the rate capability of the cells using this material as the positive electrode [16–18].

The difficulty in synthesizing stoichiometric $LiNiO_2$ is also due to the loss of lithium from the host structure during high temperature calcinations because of the high vapor pressure of lithium [17], thus leading to the formation of non-stoichiometric $[Li_{1-x}Ni_x]_{3a}[Ni_{1-x}]_{3b}[O_2]_{6c}$ structure. This results in a lower initial capacity as well as severe capacity loss upon cycling. Another problem is that capacity fade is observed even for stoichiometrically pure $LiNiO_2$, which is due to the formation of inactive NiO_2 phase due to the irreversible phase transitions occurring in $LiNiO_2$ structure when charging (de intercalation of Li^+) up to a high voltage (>4.0 V vs. Li). Hence for these reasons, $LiNiO_2$ is represented as Li_xNiO_2 where x in this case indicates the non-stoichiometry in lithium.

A qualitative picture on the battery activity can be obtained from the nature of the PXRD patterns of Li_xNiO_2. Typical XRD of $LiNiO_2$ has been represented in Fig. 2. The (*003*) peak occurs from the diffraction of layered rock-salt structure *R-3m*, whereas the (*104*) peak appears from both the diffractions of layered and cubic rock-salt structures [16]. So if Li^+ and Ni^{3+} ions are mixed completely, the intensity of (*003*) reflection should be zero resulting in an electrochemical inactive phase of $Li_2Ni_8O_{10}$ (Chart 1. JCPDS #: 23-0362).

Ohzuku et al. [19] have evaluated the crystal quality of the synthesized $LiNiO_2$ by measuring the integrated intensity ratio of (*003*) and (*104*) peaks and reported that the decrease of the $I_{(003)}/I_{(104)}$ ratio (R) indicates the formation of the cubic $LiNiO_2$ structure due to the displacement of nickel ions in to the lithium layer. According to them, the samples with $I_{(003)}/I_{(104)}$ ranging from 1.32 to 1.39 exhibit high electrochemical activity. The authors also assume that the exact chemical composition of the compound i.e. x, is not the main factor in determining its electrochemical performance when the Li/Ni ratio is close to unity, and therefore, they rely on the XRD and electrochemical characterization to control the preparation conditions. However, Moshtev et al. [20] have revealed a clear linear dependence of $I_{(003)}/I_{(104)}$ with x in the $0.91 < x < 0.99$ range (Chart 3).

Likewise, Nitta et al. [21] have reported that the integrated intensity ratio of (*006*) and (*101*) peaks should be less than 1.0, in order to obtain better electrochemical properties from the synthesized $LiNiO_2$. In addition to the above fact, it is interesting to observe that the displacement between Ni^{3+} ions at the octahedral *3b* sites and Li^+ ions at the *3a* sites in the space group *R-3m* weakens the intensity of the (*003*), while such a displacement did not affect the intensity of the (*104*) line [22]. Actually, increasing amount

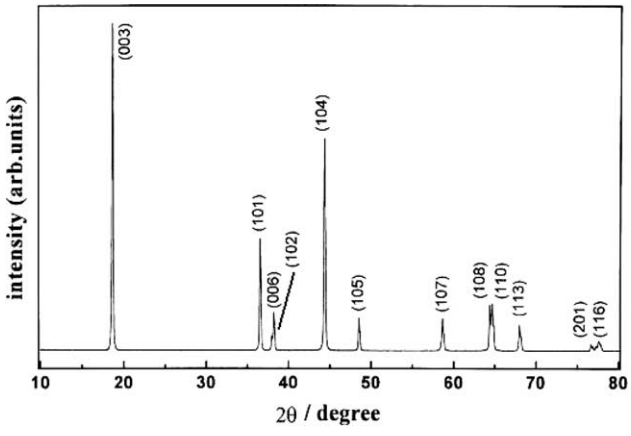

Fig. 2. Typical XRD of $LiNiO_2$. $a = 2.88$ Å, $c = 14.19$ Å; JCPDS # 9-063; Rhombohedral structure (*R-3m* -D^5_{3d}). Ref.: Lee et al., Solid State Ionics 118 (1999) 159.]

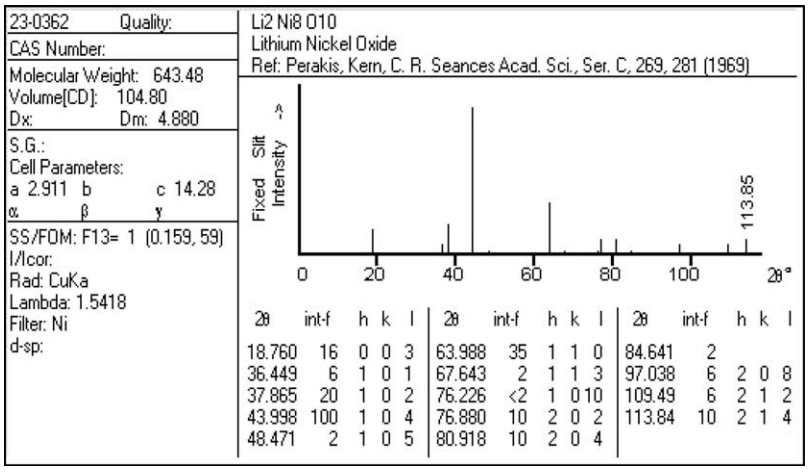

Chart 3. JCPDS data of $Li_2Ni_8O_{10}$ (#23-0362) '©JCPDS—International Centre for Diffraction Data. All rights reserved' Courtesy: ICDD, publishers of the Powder Diffraction File™, 12 Campus Boulevard, Newtown Square, Pennsylvania, USA and Perakis, Kern, C.R. Seances Acad. Sci. Ser. C, 269, 281 (1969).

of lithium in Li_xNiO_2 ($x>1$) reduces the oxidation state of nickel from Ni^{3+} to Ni^{2+}, and therefore, the lattice constant a increases slightly from 14.19 to 14.205 Å. This might cause an elongation of c-axis, because the ionic size of Ni^{2+}(0.83 Å) is larger than that of Ni^{3+}(0.70 Å) [23].

Generally, the non-stoichiometry of lithium nickelate ($Li_{1-x}Ni_{1+x}O_2$) results from the instability of trivalent Ni ions during the high temperature synthesis of the compound. Obviously, irrespective of the experimental conditions, divalent nickel ions are always present wherein half of them are situated in the lithium sites within the inter slab space [18]. However, the systematic study of preparation conditions by Rougier et al. [18] has enabled the possibility of obtaining a quasi-2D material with $x=0.014$. The amount of extra Ni ions was precisely deduced from accurate Rietveld refinement procedures, using the sensitivity of the thermal factor of lithium to the electronic density. Moreover, the magnetic property study can also be used to quantify the amount of extra nickel ions in the lithium site [18].

The existence of extra nickel ions in the lithium sites coupled with the lithium deficiency requires the presence of $2z$ divalent and $(1-z)$ trivalent nickel ions in the structure. Owing to steric considerations ($r_{Ni3+}=0.56$ Å, $r_{Ni2+}=0.68$ Å, $r_{Li+}=0.74$ Å) the nickel ions situated in the lithium layer are assumed to be divalent, leading to the $Li_{1-z}Ni^{II}_z[Ni^{III}_{1-z}Ni^{II}_zO_2]$ formula. This point is very important in understanding the magnetic properties.

Hirano et al. [24] have analyzed the decomposition mechanism of $LiNiO_2$ to proceed in three steps. According to them, it starts from the fully disordered rock-salt structure, through $Li_{1-x}Ni_{1+x}O_2$ with partially disordered α-$NaFeO_2$ structure, and a two-phase region consisting of $Li_{1-x}Ni_{1+x}O_2$ and $Li_xNi_{1-x}O$ phases. However, the decomposition reaction (reduction from Ni^{3+} to Ni^{2+}) was greatly suppressed when higher oxygen partial pressure is present during the material synthesis.

1.2. Crystallization mechanism of $LiNiO_2$

The initial heating (~400 °C) of reaction mixtures, say LiOH–$Ni(OH)_2$, is assumed to result in Li_2O and NiO—the active ingredients of $LiNiO_2$ formation. When the calcination temperature is increased to about 600 °C, a solid solution of composition $Li_xNi_{2-x}O_2$ is formed. Obviously NiO from $Ni(OH)_2$ (or nickel nitrate) has formed at this temperature, with Li^+ ions substituting for Ni^{2+} ions in NiO. When the temperature is raised to 700 °C or higher, the lithiation of NiO continued. Thus, the amount of $Li_xNi_{2-x}O_2$ phase increased accordingly, which will be confirmed from the appearance of the (*003*) Bragg peak and the increase in the intensity of the other XRD peaks. When more Li ions are incorporated into the NiO lattice, Ni^{3+} and Li^+ ions tend to occupy the O_h sites and form alternate layers between the closest packed oxygen arrays. The addition of Li ion in to NiO can be viewed as the redistribution of Li and Ni ions. Also the peaks of $Li_xNi_{2-x}O_2$ shift to higher 2θ after the temperature is increased from 700 to 750 °C or so. This result is attributed to the insertion of Li^+ ions in to the NiO lattice, which causes a reduction in the lattice constant.

The incorporation of Li into NiO lattice results in the filling of Li ions and the oxidation of Ni^{2+} to Ni^{3+} in the cation sub-lattice. The ionic radii of Li^+, Ni^{2+} and Ni^{3+} for O_h coordination are 0.76, 0.69, 0.50 Å respectively. After the filling of Li and the subsequent oxidation of Ni^{2+}, the average cationic radius is expected to be smaller ($r_{Li+}+r_{Ni3+}<r_{Ni2+}$). Thus, the lattice constant of $Li_xNi_{2-x}O_2$ decreases with the increasing time [24]. Hence, it is understood that the heating temperature, duration, and atmosphere are controlled critically, especially for the synthesis of $LiNiO_2$. Also the rate of cooling is maintained to be slow (1 °C/min or lesser) in order to avoid cation mixing in $LiNiO_2$.

1.3. Vibrational spectroscopic analysis

1.3.1. Fourier Transform InfraRed (FTIR) spectroscopy

Generally, the FTIR spectroscopic data of LiM_xO_y reveal the local structure of the oxide lattice constituted by LiO_6 and MO_6 octahedra. It is well known that the relative IR absorbance is sensitive to the short-range environment of oxygen coordination around the cations in the oxide lattices, crystal geometry and the oxidation states of the cations involved and is less likely to get affected by the grain size and the morphology or long-range order of the crystal lattice [25]. Moreover, it is generally not possible to assign specific IR frequencies to vibrations involving a single cation and its oxide neighbors [26], as the resultant vibrations of any transition metal oxide involve contributions from all possible atoms. Therefore, it is only the differences in mass, charge and co-valency of lithium and the transition metal cation that leads to the motion of lithium ion and the observation of respective vibrational spectrum [27]. It is worth recollecting the fact that the resonance frequencies of the alkali metal cations in the octahedral interstices (LiO_6) in inorganic oxides are located in the frequency range of 200–400 cm^{-1} [28,29].

Typical FTIR spectrum of $LiNiO_2$ synthesized from nitrate–hydrazine hydrate combustion method [29] has been depicted in Fig. 3. Based on the analysis of group theory, there are four infrared active vibrations for the D^5_{3d} group [30]. Since the LiO_2 and NiO_2 layers are separated in lithium nickelate, four vibrational bands can be identified in the range of 400–700 cm^{-1} for the NiO_2 layer and four more in the range of 200–400 cm^{-1} for the LiO_2 layer. The band observed around 540 cm^{-1} may be ascribed to the asymmetric stretching of M–O bonds in MO_6 octahedra and the other band around 450 cm^{-1} to the bending modes of O–M–O bonds [31]. In addition to these two bands, two weak bands positioned around 660 and 629 cm^{-1} are also observed, the appearance of which may be attributed to the bending modes of O–M–O bonds [32]. Peaks around 860 and 1430 cm^{-1} are observed invariably for all the compounds, an indication of the presence of Ni–O bond. Due to instrumental constraints, FTIR spectrum for $LiNiO_2$ has not been recorded below 400 cm^{-1} to investigate the vibrations of LiO_6. However, the FTIR spectroscopic observations made in the present study establish that the layered structure of $LiNiO_2$ is well preserved even at the atomic level and also demonstrate the high degree of ordering of cations.

1.3.2. Raman spectroscopy (RS)

Fig. 4 shows the Raman spectrum of $LiNiO_2$ sample synthesized by solid-state method. The spectrum is dominated by two bands positioned at about 545 and 625 cm^{-1} (weak compared to that of the analogous $LiCoO_2$). The factor-group analysis of D^5_{3d} yields that the $(2A_{2u}+2E_u)$ modes are infrared active and the $(A_{1g}+E_g)$ modes are Raman active [33]. The Raman band located at 545 cm^{-1} can be viewed as the symmetric O–Ni–O stretching vibration of NiO_6 units. This band is assigned to the A_{1g} symmetry in the D^5_{3d} spectroscopic space group and the RS peak at 465 cm^{-1} has the E_g symmetry.

The Raman scattering efficiency of $LiNiO_2$ appears to be very weak in comparison to the $LiCoO_2$. The origin of this feature may be due to a reduction of the rhombohedral distortion and/or an increase in the electrical conductivity in $LiNiO_2$. A reduction of the rhombohedral distortion in $LiNiO_2$ would degenerate the A_{1g} and E_g, modes of the *R-3m* symmetry into an F_{2g} mode, which is an inactive vibrational mode for the *Fm3m* symmetry of the rock-salt structure. Thus, intensities of Raman peaks are very sensitive to the long-range order in NiO_2 slabs. As pointed out by Indaba et al. [34] another reason for the decrease in intensity is an increase in electrical conductivity. It was reported that the electrical conductivity of $LiNiO_2$ is higher than that in $LiCoO_2$ because of their electronic structure [35]. The electrical conductivity of $LiNiO_2$ reduces the Raman scattering efficiency due to the weak optical skin depth of the incident laser beam. Also, the broad Raman feature of the E_g mode for $LiNiO_2$ is attributed to the tendency of non-stoichiometry as a result of the presence of an excess nickel leading to the $Li_{1-x}Ni_{1+x}O_2$ formula [36]. The departure of stoichiometry, i.e. the presence of small

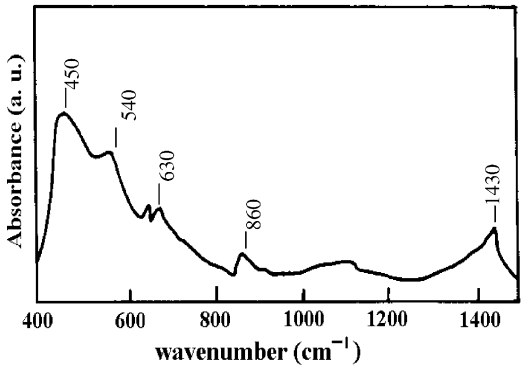

Fig. 3. FTIR spectra of $LiNiO_2$ synthesized by solution combustion method using nitrates and hydrazine hydrate fuel.

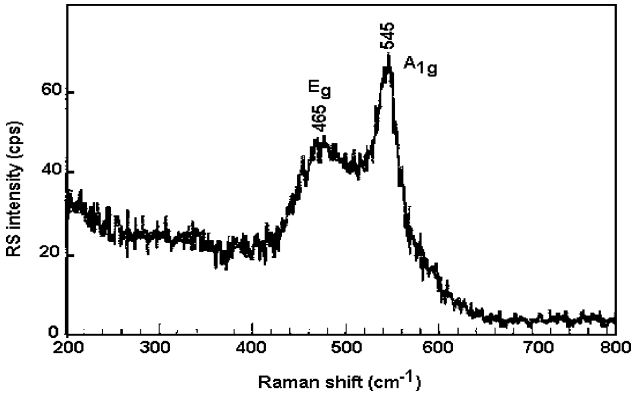

Fig. 4. Raman spectra of $LiNiO_2$. [Ref.: C.M. Julien, Mater. Sci. Engg. R 40 (2003) 47.]

amount of extra Ni that induces disorder in the Li predominant slabs is reflected in the broadening of the E_g mode.

1.4. Neutron diffraction studies

Rougier et al. [37] in their studies on $LiNiO_2$ have extracted the lithium isotropic thermal factor [B(Li)−1.2 $Å^2$) (assuming α-$NaFeO_2$ 2D structure for $LiNiO_2$) from the X-ray pattern and from this, the electronic density (Fourier Transform of the structure factors) was deduced. The difference in the electronic density between the experimental and calculated one shows the existence of a residual electronic density on the lithium site. The residual electronic density increases from 1.7 $Å^{-3}$ (for $LiNiO_2$) to 12.3 $Å^{-3}$ (for $Li_{0.80}Ni_{1.20}O_2$) when x in $Li_{1-x}Ni_{1+x}O_2$ increases. All these results show that a fraction of sites in the Li layer is occupied by nickel. Therefore, the cationic distribution can be described by two different limit models: lithium/nickel exchange with out modification of the ideal stoichiometry or the lithium deficiency phases with extra nickel ions in the lithium site leading to $Li_{1-x}Ni_{1+x}O_2$, the structure of which is given in Fig. 5.

The low scattering power of lithium, as compared to nickel, does not allow one to detect a small amount of lithium in the Ni layer from XRD studies. On the other hand, neutron diffraction studies help to get some clear picture on the above-discussed subjects. Neutron diffraction studies by Pouillerie et al. [38] have shown that the cationic distribution of the $Li_{1-x2}Ni_{1+x}O_2$ phases (typically for $x=0.02$ and 0.07) is characterized by the presence of x nickel ions in the lithium sites. There is no Li/Ni exchange between the slabs and the interslab spaces. For these compositions, the larger Li^+ ions are destabilized in the smaller octahedral sites of the NiO_2 slabs. For materials with larger departure from stoichiometry, the presence of a larger amount of Ni^{2+} ions in the slabs and in the interslab spaces lead to decreased interslab space distances and increased slab distances. Due to the instability of lithium nickel oxide at high (synthesis) temperature, fluctuations in composition would occur and the structure partially loses its anisotropy, thus resulting in a small Li/Ni mixing.

Upon de intercalation of Li_xNiO_2 and depending on the x value, a transition from the rhombohedral (hexagonal) symmetry to the monoclinic symmetry can occur ($0.25 < x < 0.55$), as indicated from XRD studies of Ohzuku et al. [39]. The phase transition occurring from hexagonal to monoclinic symmetry in $LiCoO_2$ can also be expected to occur in $LiNiO_2$, which is shown in Fig. 6. The results of neutron diffraction measurements also indicated that the disordered Ni ions situated in the Li layers are important in the appearance of monoclinic phase [40].

Also, neutron diffraction studies can be used as a tool to identify the composition of a compound as a function of inter atomic distances in $Li_{1-x}Ni_{1+x}O_2$ [40]. The Ni–O distances increase and the Li–O distances decrease with the increasing value of x, which can be explained in terms of the difference in ionic radii, r, for octahedral coordination (Ni^{3+} [low spin]: $r=0.60$ Å; Ni^{2+}: $4=0.7$ Å; Li^+:$r=0.74$ Å [41]. The Li ions at the Li site are replaced by smaller Ni^{3+} ions with the occupancy of x, and the Ni^{3+} ions in the Ni sites are reduced to Ni^{2+} ions with larger ionic radii. Ultimately, cationic disorder occurs on the octahedral sites, which lead to a shorter Li–O (2 Å when $x=0.3$) and longer Ni–O distances (2.1 Å when $x=0.3$).

1.5. Electronic structure through XANES

It is well accepted that during the course of Li de intercalation from $LiNiO_2$, a modification in electronic structure occurs. Change in electronic structure by lithium de intercalation in $LiNiO_2$ was investigated by Ni *L*-edge and O *K*-edge X-ray absorption near edge spectrum

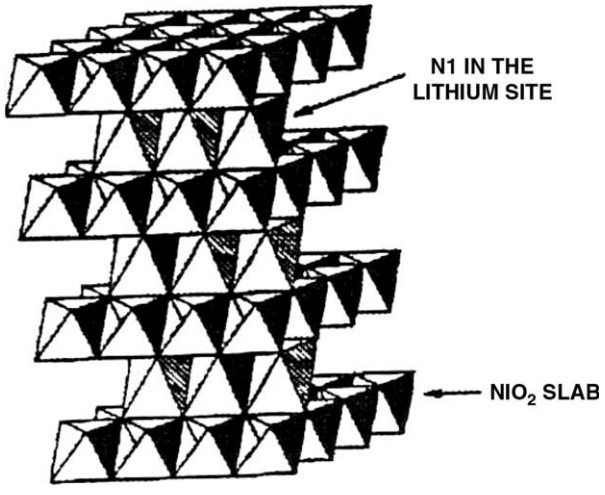

Fig. 5. A view of the $Li_{1-x}Ni_{1+x}O_2$ structure.

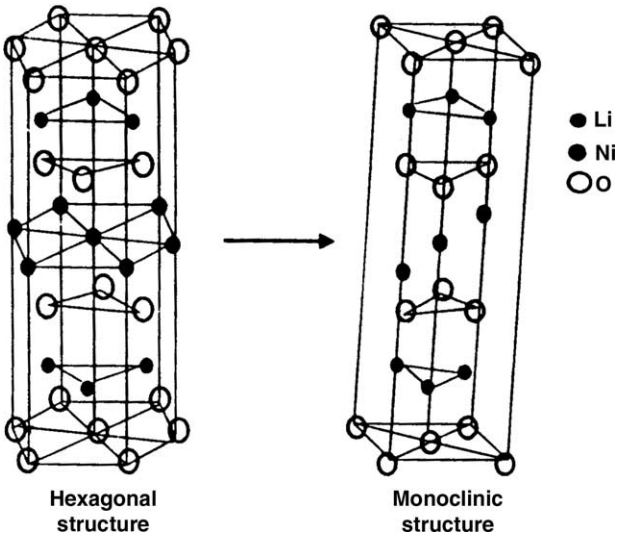

Fig. 6. Reversible phase transition between hexagonal and monolcinic structures monoclinic structure in $LiNiO_2$ ($045 \leq x \leq 0.55$).

(XANES) by Uchimoto et al. [42]. The Ni *L*-edge (Ni 2p) XANES for Li_xNiO_2 shows two strong absorption features which are similar to those of NiO, thus implies that the Ni ions in $LiNiO_2$ are Ni^{2+} ions in a high spin state. The spectra for the de intercalated phases of Li_xNiO_2 ($x=0.2$, 0,4 …, 1.0) do not exhibit chemical shift in the XANES and the changes in shape are also small, an indication that the Ni ion in the Li_xNiO_2 is still Ni^{2+} even at as low an x value as 0.2.

The O *K*-edge XANES for several de intercalated Li_xNiO_2 phases features an absorption at 533 eV, which is attributed to the band derived from the mixing of Ni 3d states with O 2p states. Similarly, the broad structure near 535–550 eV is attributed to the Ni band with 4sp character. Also, the intensity of the peak at 528 eV increased with decreased lithium content. This result shows that oxidation influences the oxygen 2p orbital, and therefore, the ground state of Li_xNiO_2 is $Ni^{2+}L$, where L represents a ligand hole state. Thus, it is understood that the lithium de intercalation reaction does not involve nickel, but oxygen, thus corroborating the results from the first principle calculations for Li_xNiO_2 systems [43–45].

Recently, first principle molecular orbital calculations of the electronic structure of $Li_{1-x}NiO_2$ have indicated that lithium ion de intercalation increases the covalent interaction between nickel and oxygen and also that the oxidation associated with the de intercalation mainly takes place on oxygen [43–45]. The choice of anion and the coordination of Li^+ with this anion have the largest effect on the lithiation voltage. This is due to the fact that the largest anion increases the electronic exchange, which happens efficiently when Li^+ intercalation is around oxygen ions. Thus, the oxygen ion, rather than the transition metal is the net acceptor of electronic charge upon lithiation.

1.6. Electrical properties

The compounds of lithium nickel oxide are usually deficient in lithium and correspondingly rich in nickel i.e., $Li_{1-x}Ni_{1+x}O_2$ ($0<x<0.25$). The excess nickel (actually Ni^{2+}) substitutes for lithium and occupies the position of Li ions. $LiNiO_2$ undergoes a phase change from a hexagonal to cubic phase at a specific temperature and the phase change is irreversible [46]. Thus, if $LiNiO_2$ is sintered at a temperature higher than the phase transition temperature (ca. 720 °C), it will contain certain amount of inactive cubic phase leading to a reduction in the electrochemical capacity ultimately. While heating at high temperatures, nickel ions in *3b* sites could obtain enough energy to leave their own O_h sites to occupy the empty *3a* O_h sites. Since Ni^{3+} ions in $LiNiO_2$ have a low spin configuration, electrons in e_g orbitals can take part in the conduction mechanism through 90° by overlapping of Ni–O–Ni atoms. It is obvious that the movement of Ni^{3+} ions from nickel layer in *3b* sites will destroy this exchange of Ni–O–Ni. Consequently, the mobility of conduction electron will largely be reduced, leading to a decrease in the conduction.

Temperature dependent electrical conductivity studies on $Li_{1-x}Ni_{1+x}O_2$ show that with the increasing x (increasing Ni^{2+} concentration at lithium positions), the electrical conductivity decreases i.e. the structural disorder related with the presence of Ni^{2+} on lithium positions causes a deterioration of electron transport in $Li_{1-x}Ni_{1+x}O_2$. This is confirmed from the electrical conductivity activation energy values (of carrier mobility) obtained from a series of $Li_{1-x}Ni_{1+x}O_2$ with varying x values. Activation energy is expected to increase with the increasing value of x i.e., with increasing nickel disorder [47]. Therefore, in order to obtain $LiNiO_2$ with acceptable electrochemical properties, x in $Li_{1-x}Ni_{1+x}O_2$ should be as minimum as possible and the temperature of synthesis of the nickel oxide materials should be below 720 °C. Thus, it is highly obvious that synthesis conditions hold the key to these parameters. For e.g., at 30 °C, the conductivity of $Li_{0.61}Ni_{0.96}O_2$ was found to ca. $2\times10^{-1}\ \Omega^{-1}\ cm^{-1}$ as reported by Rougier et al. [37].

1.7. Magnetic properties

In the rhombohedral structure of $LiNiO_2$ (*R-3m*, Li at *3a* and Ni at *3b site*), the NiO_6 octahedra of trigonal symmetry share their edges to form a triangular Ni-lattice such as depicted in Fig. 1. Since the inter-Ni sheet distance (4.37 Å) is much longer than the intra-sheet Ni–Ni distance (2.88 Å), magnetic correlations have been considered two-dimensional (2D) in nature (Ref. [49]). Further, it is seen that the synthesis of $LiNiO_2$ with reproducible electrical/electrochemical properties is a problem because the real formula of the oxide is $Li_{1-x}Ni_{1+x}O_2$ ($0<x<0.25$). Deviation from the ideal stoichiometry is connected with the ubiquity of cation mixing, primarily due to the presence of Ni^{2+} ions at the Li^+ and Ni^{3+} positions because of the similarity in their ionic sizes [48,49]. The cation mixing in turn reduces the application properties of the cathode material because the presence of Ni^{2+} ions at the lithium positions hinders Li^+ ion diffusion. Therefore, the study of the magnetic properties of these materials can be an elegant way to detect the presence of extra nickel ions in the inter slab space. Thus, as reported by Goodenough [50], the presence of extra nickel ions in the Van der Waals space drastically modifies the magnetic properties of these materials by introducing a strong coupling between the adjacent NiO_2 slabs. This leads to a change in the magnetic properties from antiferromagnetic to ferromagnetic [51]. The tendency to shift towards ferri magnetism increases with the increasing content of additional nickel ions in the lithium layers. However, anomalies are observed from sample to sample and this is due to the difficulties in obtaining ideal sample of layered $LiNiO_2$ without cation mixing. The small excess of Ni ions in the Li layers seems to significantly affect not only the magnetic properties, but also the electrical properties

namely the motion of intra layer Li ions. In this situation, NMR measurements were performed to investigate the motion of Li ions in these oxides.

Temperature dependant NMR measurements of ^{7}Li nucleus carried out over a temperature range of 77–680 K at 10.08 MHz for sample of $LiNiO_2$ suggests that a distinct relaxation process other than the ion hopping mechanism contributes to the relaxation rate ($1/T_1$) in the low temperature region. This would be due to the magnetic contribution from the Ni electron spin, which dominates the magnetic properties of $LiNiO_2$. It is also considered that at low temperatures, Ni^{3+} ions with the spin state $S=1/2$ cause the fluctuating field at Li sites through the transferred hyperfine interaction via Li(2s)–O(2p)–Ni(3d) bonds and hence affects the relaxation rate for ^{7}Li nucleus. Various experiments including specific heat and susceptibility measurements indicate that the intrinsic nature of triangular lattice anti-ferromagnetism appears and some kind of magnetic ordering occurs in the low temperature region below 50 K. For e.g., Kitaoka et al. [52] have pointed out that local short-range ordering like ferromagnetic spin-glass behavior is caused by imperfection in $LiNiO_2$. However above 50 K, $LiNiO_2$ shows a behavior typical of para-magnetic substances. Thus, the magnetic relaxation process arising from Ni^{3+} spins, which is dominant at low temperatures, changes into a relaxation process based on the motion of Li^+ defects with the increasing temperature. In a Li deficient sample like $Li_{0.5}NiO_2$, a part of Ni^{3+} ions would change into non-magnetic Ni^{4+} ions ($S=0$), influencing the relaxation rate as a result of decreased Ni^{3+} ions concentration. Hence, from the ^{7}Li relaxation rate measurements, one can indirectly identify the presence of Ni^{2+} in the lithium layers of Li_xNiO_2.

1.8. Thermal stability

Thermal behavior of Li_xNiO_2 electrodes has been of great interest because it affects the battery safety [53,54]. The thermal behavior of the materials is usually studied using thermogravimetry (TG) or differential scanning calorimetry (DSC) and the decomposition mechanism is investigated by employing X-ray diffraction technique on the thermally decomposed products. $LiCoO_2$, $LiMn_2O_4$ and $LiNiO_2$ are all stable in air even at high temperatures. By contrast, Li_xCoO_2, $Li_xMn_2O_4$ and Li_xNiO_2 ($x<1$), which are produced by lithium extraction from $LiMO_2/LiM_2O_4$, are meta stable and liberate oxygen in the electrolyte (when they are heated in non-oxidant atmosphere). The temperature at which O_2 evolution occurs depends on x and on the nature of the material. The amount of O_2 released on heating increases as x decreases in Li_xNiO_2, and therefore, it is important to keep x from getting too small. In a recent work, Mc Breen et al. [55] studied the thermal behavior of $Li_{x-y}Ni_{2-x}O_2$ samples made initially from $Li_xNi_{2-x}O_2$ where x is 0.77 and the values of y ranging from 0 to 0.5. For $0<y<0.4$, the materials get decomposed, liberating O_2 above 400 °C. For $0.4<y<0.5$, a significant weight loss was seen near 250 °C. This is believed to be associated with the release of O_2 necessary for the formation of a spinel phase related to $LiNi_2O_4$ [56]. Basically, prior to the process of heating, the lithium in $LiNiO_2$ forms an ordered state. When heated above 180 °C or so, three fourths of Ni remains in the nickel layers and one fourth moves predominantly to the lithium layers. This arrangement occurs with an exothermic process. However, it takes longer time to achieve a complete spinel structure, as reported by Kanno et al. [57]. For $y<0.4$, no oxygen release was observed at 250 °C and no spinel phase is formed. Above 400 °C, all samples of $Li_{x-y}Ni_{2-x}O_2$ were thought to undergo the following reaction when heated above 400 °C.

$$Li_{x-y}Ni_{2-x}O_2 \rightarrow Li_{x-y}Ni_{2-x}O_{2-y} + (y/2)O_2$$

$Li_{x-y}Ni_{2-x}O_{2-y}$ is a member of the rock-salt related solid solution $Li_xNi_{2-x}O_2$, which has equal numbers of cations and anions. $Li_{0.77}Ni_{1.23}O_2$ [30] has substantial amounts of nickel atoms in the layers normally occupied only by lithium in $LiNiO_2$ (random cation mixing). This causes a disorder in its crystal structure, which is accompanied by an exothermic reaction. These misplaced nickel atoms significantly reduce the specific capacity of the electrode materials and such materials are, therefore, not generally used in practical Li cells. The stability of Li_xNiO_2 is lower than that of $LiCoO_2$ because Ni^{3+} is more readily reduced than the cobalt counterpart. These results suggest that it will be difficult to make cells based on $LiNiO_2$ to operate satisfactorily at high temperature.

1.9. Moisture stability

Due to cation mixing and other intrinsic problems, there exists an increasing amount of Ni^{2+} ions within the Vander waals gap. This reduces the amount of lithium ions in the $LiNiO_2$ structure and hence results in an inferior electrochemical capacity and rate capability of the cells when the material is used as the positive electrode. In the case of $LiNiO_2$, the degree of cation mixing in the final product was found to be strongly dependent on the water content of the initial reaction mixture. $LiNiO_2$ is not stable in water, upon heating in non-oxidant ambient and upon moisture exposure. The compound is prone to exchange with protons for Li and is readily reduced/decomposed to form $Li_xNi_{2-x}O_2$. This tendency to degradation explains the limited water content necessary to perform the $Li^+ \rightarrow H^+$ exchange reaction. Indeed this instability, compared to that of $LiCoO_2$, also explains the differences in the synthesis conditions of these two materials. Cobalt substitution in $LiNiO_2$ i.e. $LiNi_{1-x}Co_xO_2$ prevents the degradation/reduction process (i.e., formation of $Li_xNi_{2-x}O_2$) even in the presence of water [58]. Hence, oxygen atmosphere or partial cobalt substitution is needed to stabilize Ni^{3+}.

1.10. Crystal chemistry from XAFS

Rougier et al. [59] have reported for the first time the presence of an NiO_6 distortion (two different Ni–O bond lengths: four bonds at 1.91 Å and two at 2.09 Å) in $LiNiO_2$ due to the local Jahn–Teller effect of the Ni^{3+} ion, based on an X-ray absorption fine structure analysis (XAFS) analysis. It is interesting to note that the weighted average of these two distances is in the range of 1.96–1.97 Å, which is consistent with the distance based on XRD data. Crystallographically, the Ni atom is located at the *3b* site of the *R-3m* lattice with six oxygen atoms at equal Ni–O distances. Therefore, the distortion should not occur at long range and cannot be detected by conventional diffraction techniques. EXAFS, therefore, is the most suitable technique for examining local structural variations in the transition metal atoms during the charge–discharge process.

Ni K-edge EXAFS recorded as a function of x in $Li_{1-x}NiO_2$ is reported to show a peak around 1.5 Å, which is attributed to the Ni–O interaction in the first coordination sphere. The second peak around 2.4 Å represents the Ni–Ni interaction in the second coordination sphere, with some contribution from the Ni–Li interaction, although this contribution is practically negligible, because of the small backscattering amplitude of the Li atom. Also the peak at 1.5 Å could be ascribed to the Jahn–Teller distortion from the true octahedral coordination. The peak height increases with the deintercalation of lithium. It is well known that low spin Ni^{3+} is a d^7 Jahn–Teller ion with an electronic configuration of $t_{2g}^6 e_g^1$. Deintercalation of Li oxidizes Ni^{3+} to Ni^{4+}, resulting in a $t_{2g}^6 e_g^0$ state with no Jahn–Teller distortion. This is the first observation of a dynamic change in Jahn–Teller effect during the deintercalation process [60]. The existence of the Jahn–Teller effect in $LiNiO_2$ may account for the instability of $LiNiO_2$ as a cathode material. It is also observed that substitution of Ni^{3+} (d^7) in $LiNiO_2$ with Co^{3+} (d^6) causes an increase in the Ni–O peak heights, possibly reducing the Jahn–Teller effect by way of decreasing the local distortion of the NiO_2 octahedra. Consequently, the usage of $LiNi_{1-x}Co_xO_2$ as cathode materials improves the electrochemical characteristics of the battery [61]. In any case, the Jahn–Teller distortion in NiO_6 octahedron remains at the local scale [61].

1.11. Mössbauer spectroscopy

Most of the recent works deal with cationic substitution in $LiNiO_2$ in order to improve the properties of the compound. Especially, when Fe is one of the dopants in $LiNiO_2$, structural modification taking place during redox processes can also be investigated by Mössbauer Spectroscopy, in addition to XRD.

Prado et al. [62] have investigated the structural modification of quasi-stoichiometric $Li_{0.97}(Ni_{0.7}Fe_{0.15}Co_{0.15})_{1.03}O_2$ phase by XRD and Mössbauer Spectroscopy. Their XRD studies show a strong decrease of the M–O bond distance upon lithium deintercalation. While Mössbauer Spectroscopy study showed that nickel and iron are simultaneously oxidized, a large number of iron ions being stabilized in the high spin tetravalent state. They also conclude that the presence of cobalt ions facilitated the oxidation of Fe. Comparison of the average cationic charge (deduced from electrochemical study) to the number of oxidized iron (Mössbauer Spectroscopy) shows that Ni^{3+} and Fe^{3+} are simultaneously oxidized during the second step of the charge process ($0.3 \leq x \leq 0.9$). These observations suggest that oxidation of the Ni and Fe ions is easier in the Co substituted $Li_x(Ni_{0.7}Fe_{0.15}Co_{0.15})_{1.03}O_2$ system than in the $Li_x(Ni_{0.9}Fe_{0.1})_{1.01}O_2$ system or $Li_x(Ni_{1-y}Co_y)O_2$ system. The presence of a large amount of small cations (Ni^{4+} and Co^{3+}) explains why it is easier to oxidize iron ions in the $Li(Ni,Co,Fe)O_2$ phase than in the $Li(Ni,Co,Fe)O_2$ phase.

1.12. Electrochemistry of $LiNiO_2$

During the charge process, the trivalent nickel ions in the low spin configuration ($t_6^2 e^1$) are oxidized to the low spin tetravalent state (t_6^2). Total reversibility of the first cycle is an indicative of the stoichiometric compound with negligible Ni(II) in the lithium layer. However, the formation of low lithium content Li_xNiO_2 ($x < 0.2$) causes cycle life failure. In addition, the material become highly catalytic toward electrolytic oxidation, and some of the nickel ions may migrate to lithium sites. The formation of pure $LiNiO_2$ is thus difficult, and residual Ni(II) (up to 1–2%) exists between the NiO_2 slabs. Essentially, the first cycle irreversibility during charge–discharge is related to the amount of Ni(II) between the slabs of NiO_2, which require extra charge for oxidation to higher valence state, when electrolyte decomposition is controlled [63].

Good cycling properties with reversible capacities in the 150–160 mAh/g range have been achieved with $LiNiO_2$ with small degrees of non-stoichiometry. Moreover, the overall reversible specific capacities reported for $LiNiO_2$ are typically 10–30 mAh/g higher than those for $LiCoO_2$, despite their same theoretical capacity of about 274 mAh/g. These aspects make $LiNiO_2$ particularly attractive as cathode materials in lithium batteries. However, the electrostatic repulsions between the lithium ions and the extra nickel ions and the interslab space narrowing resulting from the presence of divalent or trivalent nickel ions limit considerably the reversibility of lithium cathodes, when the composition of the starting lithium nickelate is too far from the ideal one [4]. Therefore, an intense care becomes highly essential in synthesizing $LiNiO_2$ with exact stoichiometry, which requires controlled synthesis atmospheric conditions.

During the deintercalation of lithium ions from $LiNiO_2$, a decrease in a value and an increase in the c value were observed [47]. The process of de intercalation modifies the electronic structure of the cathode material, which in turn renders a metallic character to the deintercalated phases.

Interestingly, an increased ionic–electronic transport condition is established due to the increased lithium chemical diffusion with decreasing lithium concentration in $LiNiO_2$.

Though $LiNiO_2$ exists in two structural modifications viz., cubic and layered hexagonal, it is well admitted that only the hexagonal phase is electrochemically active [64]. Regarding the phase transition phenomenon of Li_xNiO_2 is concerned, hexagonal and monoclinic phases are observed to co-exist around $x=0.2$ and a monoclinic phase exists for $0.25<x<0.50$. Another two-phase region in which a monoclinic phase and hexagonal phase coexist appears for $0.50<x<0.57$ [65]. The transition from the hexagonal to monoclinic structure is depicted in fig. 5. It has been shown that the capacity of $LiNiO_2$ depends strongly upon the structure parameters, while these parameters are closely related to the synthesis conditions [66].

In general, the Li^+ intercalation/deintercalation mechanism may be understood from cyclic voltammetric studies [67]. It is interesting to note that the mechanism of Li intercalation/deintercalation is quite different for $LiNiO_2$ and $LiCoO_2$. The first charge and discharge curve of a $LiNiO_2$ cathode is totally different from the subsequent cycles. The Li from $LiNiO_2$ cannot be fully re-inserted during the subsequent reduction step due to the structural transformation to $Li_{1-x}NiO_2$. After a few cycles, the reversible reaction can be described as follows:

$$Li_{0.85}NiO_2 \leftrightarrow Li_{0.35}NiO_2 + 0.5Li^+ + 0.5e^-$$

The practical specific discharge capacity of $LiNiO_2$ is about 125–150 mAh/g [67]. Contrary to these observations, in the case of $LiCoO_2$, the lithium after the first charging process is completely re-inserted during the following discharge process [41].

It is also considered that the increase of lithium content in Li_xNiO_2 decreases the oxidation state of some Ni ions from Ni^{3+} to Ni^{2+}, which might increase the formation of an electrochemically inert phase in the $LiNiO_2$ since Ni^{2+} has a more stable state [68]. This may impede the motion of the lithium ions leading to the deterioration of the electrode during charge and discharge. In this regard, Yamada et al. [69] measured the initial discharge capacity as a function of average oxidation state of Ni in $LiNiO_2$ materials. They observed that the initial discharge capacity was the highest when the oxidation state of nickel ion was 3.0, corresponding to the high crystal quality of $LiNiO_2$. The capacity fade in Li_xNiO_2 is, therefore, considered to be due to the destruction of the NiO_2 layer in the $LiNiO_2$ crystal by the extraction of lithium ions during the charging process, as observed from the structural analysis by Li et al. [65]. During the process of charging, they observed that $LiNiO_2$ shows a sequential change in crystal structure from the hexagonal phase (H1) to the monoclinic phase (M1), the hexagonal phase (H2) again, then two hexagonal phases (H2 + H3) and finally to a single hexagonal phase (H3) [70]. The second hexagonal phase that has appeared in the two regions causes the sudden decrease in the *c*-lattice parameter that leads to the shrinkage of the crystal lattice. Also, it is suggested that the crystal lattice shrinkage may deform the NiO_2 layer in the $LiNiO_2$ crystal lattice and such a deformation may result in an irreversible structural change.

The disordered region also prevents the extension and reduction of the interlayer distance between NiO_2 sheets. Consequently, the nickel ions in the lithium sheet including near neighbors are inactive for the electrochemical reaction. This is the reason why the samples having high concentration of nickel ions at lithium sites are inactive in non-aqueous lithium cells [70].

Hence, various complications related to the synthesis of $LiNiO_2$ can be summarized as follows:

- Difficulties in stabilizing Ni^{3+} (deviation from rhombohedral structure).
- Requirement of stringent synthesis conditions (requires O_2 atmosphere).
- Presence of off-stoichiometry and cation-mixing.
- Irreversible phase transitions during electrochemical cycling. Unavoidable Li–Ni disorder.

Since $LiNiO_2$ is associated with above detrimental factors, which are the prime reasons for the degraded electrochemical performance, various parameters that are related to the preparation conditions need to be controlled especially to get an electrochemically active material. Through careful synthesis and adjustment of lithium concentration during the heat-treatment, a near stoichiometric $LiNiO_2$ could be obtained. In this context, several methodologies have been followed to obtain $LiNiO_2$ cathodes with high degree of purity and crystallinity with an intention of achieving good degree of electrochemical performance. The most studied and established procedures, which are being adopted to synthesize these oxide cathodes with better battery activity, are described in this section. It is worth mentioning that these procedures, known for their high degree of flexibility and viability, may be employed to synthesize a variety of other potential cathode candidates also. Certain important reported procedures for the synthesis of $LiNiO_2$ involving solid-state and wet-chemical routes are given below.

1.13. Synthesis of $LiNiO_2$

Solid-state method. Nagayama et al. [71] have extensively studied the synthesis of $LiNiO_2$ using several combinations of hydroxides and carbonates as lithium and nickel sources. From the electrochemical behavior of the synthesized compounds, $LiNiO_2$ prepared by heat-treating lithium and nickel hydroxides for 750 °C in O_2 atmosphere exhibited a discharge capacity of around 190 mAh/g.

Generally, in the solid-state route, a number of precursor combinations such as oxides, hydroxides, carbonates, acetates etc., may be employed. But all those combinations

may not yield $LiNiO_2$ with better electrochemical performance. Therefore, the selection of precursors is as important as optimizing the heat-treating temperature, dwelling time, heating atmosphere, etc.

Microwave-assisted synthesis. An ever first attempt on the synthesis of $LiNiO_2$ using microwaves has been made by the authors of the present communication and an elaborate discussion regarding the synthesis procedure and the evaluation of electrochemical performance of the same has been described elsewhere [72]. In the study, the possibility of synthesizing $LiNiO_2$ using microwave radiation and to optimize the irradiation time and post-heat treating conditions required for the formation of phase pure $LiNiO_2$ with acceptable electrochemical characteristics have been explored. An extensive study in understanding the effect of microwaves on various possible precursors, microwave exposure times were carried out. Precursors of lithium and nickel, combinations of hydroxides, carbonates and oxides of lithium and nickel have been selected for the present study to synthesize $LiNiO_2$ using microwaves. Table 1 shows the combinations of different precursors employed in this regard. It is noteworthy from the experimental observation that among the various precursor combinations attempted to synthesize $LiNiO_2$ by microwaves, all the combination except Li_2CO_3—basic nickel carbonate are found to be microwave receptive in nature. Pellets were made out the precursors and are exposed to microwave for 3, 5, 7 and 15 min separately.

Normally, the reaction was found to get triggered after 15–20 s with the appearance of orange color glow, presumably due to the interaction of lithium ions with the microwave radiation. The disappearance of the glow was taken as the sign of completion of the reaction. Also, the study features a quotable observation that the normal procedure of intermittent grinding being practiced for any conventional method of preparation has led to insignificant interaction of precursors (invariably all the precursors chosen) with further microwave exposure. To compare the electrochemical results, $LiNiO_2$ was also synthesized by exposing the precursors to microwaves alone for 5 min (without post-heat treatment) in one attempt and by heating the products obtained as above in O_2 atmosphere at 700 °C for 5 h in another attempt. Typical electrochemical study carried out the $LiNiO_2$ sample synthesized using LiOH–$Ni(OH)_2$ precursor combination exhibited a discharge capacity of about 150 mAh/g at the end of 30 cycles. $LiNiO_2$ synthesized using the same precursor with subsequent post-heat treatment in O_2 for 5 h preceded by microwave exposure for 5 min exhibited superior electrochemical performance. A discharge capacity value of about 160 mAh/g (after 30 cycles) has been realized from the optimized synthesis condition. Besides being simple in nature, this specific method is bestowed with significant advantages that include cost-effectiveness and energy efficiency. Also, the electrochemical performance of the products was found to be comparable with that of the conventional ceramic route. Therefore, the highlight of this method is that a combination of microwave irradiation without intermittent grinding and a post-heat treatment has been found to be preferable and time conserving than the prolonged conventional furnace heating (at least 20 h) procedures.

Table 1
Combinations of precursors chosen for microwave—assisted synthesis of $LiNiO_2$

Label	Lithium source	Nickel source	Interaction with microwaves
[A]	LiOH	$Ni(OH)_2$	Positive
[B]	LiOH	Ni_2O_3	Positive
[C]	LiOH	Basic nickel carbonate	Positive
[D]	Li_2CO_3	$Ni(OH)_2$	Positive
[E]	Li_2CO_3	Ni_2O_3	Positive
[F]	Li_2CO_3	Basic nickel carbonate	Negative

Pechini method. $LiNiO_2$ was prepared by using citric acid, ethylene glycol and nitrates of lithium and nickel. The metal ions form chelates with citric acid and glycol, which turns in to a gel upon heating around 80–90 °C. The gel was calcined from 400 to 800 °C for 12 h in air or O_2 atmosphere. Stoichiometric $LiNiO_2$ was reported to be obtained only when the sample was heat-treated in oxygen atmosphere. Crystallization mechanism of $LiNiO_2$ synthesized by this method has been studied in detail and the report does not contain the results of the electrochemical studies of this compound [73].

Acid-assisted sol–gel method. Acetates of lithium and nickel were dissolved in de-ionized water and the dissolved solution was added drop by drop into a continuously stirred aqueous solution of adipic acid, which is used for chelating the metal ions. The molar ratio of adipic acid and the acetates was set as unity. Also, the pH of the solution was adjusted to be in the range of 2.5–3.5 by adding acetic acid. The solution, thus, obtained was evaporated at 80 °C for 5 h, when transparent sol was obtained. As evaporation continued the sol turns into a viscous gel, which was slowly heated to 750 °C in flowing O_2 for 14 h [74]. A capacity of about 160 mAh/g was observed for first few cycles and capacity fading was observed as cycling progressed.

Combustion method. By combustion method, Mohan Rao et al. [75] for the first time have synthesized $LiNiO_2$ using nitrate as the cation source and stoichiometric amount of urea as the fuel at a moderate temperature of about 500 °C. Though, the PXRD pattern showed a perfect matching with the JCPD standard pattern, the intensities of the Bragg peaks (especially of (*003*) and (*104*) peaks) were inconsistent with those observed for the standard, thereby resulting in a compound of composition $Li_{1-x}NiO_2$ with $x=0.4$. As the study was oriented towards the application of the synthesized $LiNiO_2$ (necessarily $Li_{1-x}NiO_2$) in aqueous battery systems, there was no

Table 2
Precursors and fuels used in combustion route and the basis of selection

Fuel	Type of fuel	Basis	Heat treatment[a]	Reference
Urea	Carbo-nitrogenous	$\varphi_e = 1$	400 °C 30 min and 700 °C 15 h	[7]
Glycine	Carbo-nitrogenous	$\varphi_e = 1$	-do-	[8]
Gelatin	Carbo-nitrogenous	Trial and error	700 °C 15 h	[8]
Starch	Carbonaceous	Trial and error	-do-	[9]
Hydrazine hydrate	Nitrogenous	Trial and error	-do-	[8]

[a] Thermal treatment in flowing O_2 atmosphere.

mention about the electrochemical characteristics of the same compound in the non-aqueous lithium batteries.

Therefore, investigation was undertaken by the authors of the present communication essentially with a view to synthesize phase-pure $LiNiO_2$ by combustion method using urea and some other novel fuels and to evaluate the electrochemical behavior of the samples for use in non-aqueous lithium batteries. The actual procedure adopted and the optimized synthesis conditions followed to synthesize the oxide cathodes are described in Ref. [76] in a detailed manner.

In this method, using nitrates as the cationic source, various combustion aiding organic fuels (classified as carbonaceous, nitrogenous and carbo-nitrogenous, based on the major constituents present) have been employed to synthesize $LiNiO_2$. The amount of fuel required for the synthesis of $LiNiO_2$ has been fixed either from the equivalence ratio φ_e, i.e. the ratio of the oxidizing valency of metal nitrates to the reducing valency of the fuel equaling to 1 [77] or by trial and error method. Table 2 lists out various types of fuels employed in the synthesis of $LiNiO_2$, the basis of selection and the heat treatment involved in the procedure. The study suggests solution based combustion method involving hydrazine hydrate fuel to synthesize electrochemically better performing $LiNiO_2$ delivering an average of about 170 mAh/g as the discharge capacity at the end of 20 cycles.

Other techniques. Chemical Vapor Deposition (CVD) [78], Metallo-Organic Chemical Vapor Deposition (MOCVD) [79], Laser ablation [80] etc., are very expensive techniques and are employed particularly for fabricating thin films and coatings for fabricating semiconductor wafers and thin-film batteries.

Among the surface modification techniques adopted, substitute for Ni with an electro chemically inert cation, viz., Al, Mg, Ti or Mn has been identified to be a successful approach as far as stabilization of layered frame work is concerned. On the other hand, simultaneous doping of multiple metal ions has been claimed to offer better capacity retention and thermal stability, via., suppression of phase transitions upon cycling [81,82]. Electrochemically inactive metal oxide coating [83–85] is yet another technique which has been reported to produce $LiNiO_2$ with good capacity retention. Chowdari et al., [86] reported that TiO_2 coated $LiNi_{0.8}Co_{0.2}O_2$ material showed improvement in cycling performance which leads to an understanding that Ti doping and/or TiO_2 coating is efficient in imparting significant changes in $LiNiO_2$ and $LiCoO_2$ cathodes. In this regard, methods such as hydrolyzation combined with calcination process, citrate based sol–gel methods are reported to yield electrochemically better performing cathode products. It is noteworthy that the process of metal doping and metal oxide coating play different roles in improving the electrochemical performance of a cathode i.e., suppression of lattice changes/phase transitions and the improvement of interface stability are the underlying mechanisms of doping and coating of $LiNiO_2$ compound with metal or metal oxides, respectively [87].

2. Conclusion

In this report, the importance and significance of $LiNiO_2$ as an electrode material for rechargeable lithium cells is stressed by discussing some of the fundamental results of $LiNiO_2$ obtained by various lithium battery pioneers with an extensive research focus from different angles. This report also discussed some of the procedures that are employed in synthesizing the near stoichiometric $LiNiO_2$. The report will be helpful for developing certain other newer cathode materials of both similar and dissimilar category with disparate compositions and electrochemical features for the batteries of the future.

Acknowledgements

The authors acknowledge Dr N.G. Renganathan for his fruitful discussion and Ms P. Kalyani acknowledges CSIR, (New Delhi) India, for the award of Senior Research Fellowship.

References

[1] A.J. Salkind, Capacity of layered cathode materials for lithium-ion batteries—a theoretical study, in: A.J. Salkind (Ed.), Proceedings of the Symphosium on History of Battery Technology, Pennington, NY, 1987, pp. 87–114.
[2] D. Linden, in: D. Linden (Ed.), Handbook of Batteries and Fuel Cells, McGraw-Hill Publishing Co, NY, 1984, pp. 1.3–1.12.
[3] S. Hossain, in: D. Linden (Ed.), Handbook of Batteries, McGraw-Hill Book Co., NY, 1984, p. 63.1.

[4] E.J. Cairns, $LiNiO_2$ intercalation cathodes for lithium secondary batteries, Electrochim. Acta 41 (1994) 1459.
[5] C.F. Holmes, in: G. Pistoia (Ed.), Lithium Batteries, vol. 5, Elsevier, Amsterdam, 1994 (Chapter 10).
[6] T. Ohzuku, A. Ueda, M. Nagayama, Electrochemistry and structural chemistry of $LiNiO_2$ (R3m) for 4V secondary lithium cells, J. Electrochem. Soc. 140 (1993) 1862.
[7] N. Kalaiselvi, P. Periasamy, R. Thirunakaran, B. Ramesh Babu, T. Premkumar, N.G. Renganathan, M. Raghavan, N. Muniyandi, Iron doped lithium cobalt oxides as lithium intercalation cathode materials, Int. J. Ionics 7 (2001) 451–455.
[8] P. Kalyani, N. Kalaiselvi, N. Muniyandi, A new solution combustion route to synthesize $LiCoO_2$ and $LiMn_2O_4$, J. Power Sources 111 (2002) 232–238.
[9] P. Periasamy, N. Kalaiselvi, R. Thirunakaran, T. Premkumar, N.G. Renganathan, M. Raghavan, N. Muniyandi, Solid-state synthesis and characterization of $LiNi_yCo_{1-y}O_2$ ($0.0 \leq y \leq 0.4$), Int. J. Inorg. Mater. 3 (2001) 401–407.
[10] N. Kalaiselvi, P. Periasamy, B. RameshBabu, T. Premkumar, N.G. Renganathan, N. Muniyandi, M. Raghavan, Significance of Mg doped $LiMn_2O_4$ spinels as attract 4V cathode materials for use in lithium batteries, Int. J. Ionics 7 (2001) 187–191.
[11] P. Kalyani, N. Kalaiselvi, N. Muniyandi, Microwave assisted synthesis of $LiNiO_2$—a preliminary investigation, J. Power Sources 123 (2003) 53–60.
[12] P. Kalyani, N. Kalaiselvi, N.G. Renganathan, M. Raghavan, Studies on $Li_{0.7}Al_{0.3-x}Co_xO_2$ solid solutions as alternative cathode materials for lithium batteries, Mater. Res. Bull. 39 (2004) 41–54.
[13] J.M. Tarascon, M. Armand, Issues and challenges facing rechargeable lithium batteries, Nature 414 (2001) 361.
[14] C. Delmas, in: G. Pistoia (Ed.), Lithium Batteries, vol. 5, Elsevier, Amsterdam, 1994 (Chapter 2).
[15] H.J. Orman, P.J. Wiseman, Synthesis and characterization of $LiNiO_2$ compounds as cathodes for rechargeable lithium batteries, Acta Cryst. C 40 (1984) 12.
[16] J. Morales, C. Perez-vicente, J.L. Tirado, Cation distribution and chemical deintercalation of $Li_{1-x}Ni_{1+x}O$, Mater. Res. Bull. 25 (1990) 623.
[17] J.R. Dahn, V. von Sacken, C.A. Michal, Structure and electrochemistry of $Li_{1\pm y}NiO_2$ and a new Li_2NiO_2 phase with the $Ni(OH)_2$ structure, Solid State Ionics 44 (1990) 87.
[18] A. Rougier, P. Gravereau, C. Delmas, Optimization of the composition of the $Li_{1-z}Ni_{1+z}O_2$ electrode materials: structural, magnetic and electrochemical studies, J. Electrochem. Soc. 143 (1996) 1168.
[19] T. Ohzuku, A. Ueda, M. Nagayam, I. Iwakishi, H. Komori, Comparative study of $LiCoO_2$, $LiNi_{0.5}Co_{0.5}O_2$ and $LiNiO_2$ for 4V secondary lithium batteries, Electrochim. Acta 38 (1993) 1159.
[20] R.V. Moshtev, P. Zatilova, V. Manev, A. Sato, The $LiNiO_2$ solid solutions as a cathode materials for rechargeable lithium batteries, J. Power Sources 54 (1995) 329.
[21] Y. Nitta, K. Okamura, K. Haraguchi, S. Kobayashi, A. Ohta, Crystal structure study of $LiNi_{1-x}Mn_xO_2$, J. Power Sources 54 (1995) 511.
[22] S.P. Lin, K.Z. Fung, Y.M. Hon, M.H. Hon, Crystallization mechanism of $LiNiO_2$ synthesized by Pechini method, J. Cryst. Growth 226 (2001) 148.
[23] S. Yamada, M. Fujiwara, M. Kanda, Synthesis and properties of $LiNiO_2$ as cathode materials for secondary batteries, J. Power Sources 54 (1995) 209.
[24] A. Hirano, R. Kanno, Y. Kawamoto, Y. Takeda, K. Yamaura, M. Takano, K. Ohyama, M. Ohashi, Y. Yamaguchi, Relationship between non-stoichiometry and physical properties of $LiNiO_2$, Solid State Ionics 78 (1995) 123.
[25] S.P. Lin, K.Z. Fung, Y.M. Honn, M.H. Hon, Crystallization kinetics and mechanism of the $Li_xNi_{2-x}O_2$ ($0 < x \leq 1$) from Li_2CO_3 and NiO, J. Cryst. Growth 234 (2002) 176.
[26] R. Thirunakaran, Mg substituted $LiCoO_2$ for reversible lithium intercalation, Int. J. Ionics 9 (2003) 388–394.
[27] N. Kalaiselvi, A.V. Raajarajan, B. Sivagaminathan, N.G. Renganathan, N. Muniyandi, M. Raghavan, Synthesis of optimized $LiNiO_2$ for lithium ion batteries, Int. J. Ionics 9 (2003) 382–387.
[28] P. Kalyani, N. Kalaiselvi, N. Muniyandi, On the effects of simultaneous substitution of Al^{3+} and B^{3+} in $LiNiO_2$ cathodes, J. Electrochem. Soc. 150 (6) (2003) A759–A764.
[29] P. Kalyani, Synthesis and characterization of nickel based oxide cathodes for lithium battery applications, PhD Thesis, Submitted (2003).
[30] J. Broadhead, H.C. Kuo, in: D. Linden (Ed.), Handbook of Batteries, McGraw Hill Book Co., NY, 1984, p. 2.3.
[31] S. Hossain, in: D. Linden (Ed.), Handbook of Batteries, McGraw-Hill Book Co., NY, 1984, p. 36.13.
[32] S. Chitra, P. Kalyani, B. Yebka, T. Mohan, E. Haro-Poniatowski, R. Gangadharan, C. Julien, Synthesis, characterization and electrochemical studies of $LiNiVO_4$ cathode materials in rechargeable lithium batteries, Mater. Chem. Phys. 65 (2000) 32.
[33] R.K. Moore, W.B. White, Characterization of structure and electrochemical properties of $LiNiO_2$ cathodes for rechargeable lithium batteries, J. Am. Ceram. Soc 53 (1970) 5679.
[34] M. Inaba, Y. Todzuka, H. Yoshida, Y. Grincourt, A. Tasaka, Y. Tomida, Z. Ogumi, Synthesis and electrochemical properties of $LiNiO_2$ with nano structure, Chem. Lett (1995) 889.
[35] C. Julien, Local cationic environment in lithium nickel cobalt oxides used as cathode materials for lithium batteries, Solid State Ionics 136–137 (2000) 887.
[36] J.R. Dahn, U. von Sacken, C.A. Michal, Structure and electrochemistry of $Li_{1\pm y}NiO_2$ by X-ray diffraction, Solid State Ionics 44 (1990) 87.
[37] A. Rougier, P. Gravereau, C. Delmas, Synthesis of $LiNiO_2$ in air atmosphere: X-ray diffraction characterization and electrochemical investigation, J. Electrochem. Soc. 143 (1997) 1186.
[38] C. Pouillerie, E. Suard, C. Delmas, Structural characterization of $Li_{1-z-x}Ni_{1+z}O_2$ by neutron diffraction, J. Solid State Chem. 158 (2001) 187.
[39] T. Ohzuku, A. Ueda, M. Nagayama, Electrochemistry and structural chemistry of $LiNiO_2$ cathode, J. Electrochem. Soc. 140 (1993) 1862.
[40] A. Hirano, R. Kanno, Y. Kawamoto, K. Oikawa, T. Kamiyama, F. Izumi, Neutron d diffraction study of the layered $Li_{0.5-x}Ni_{1+x}O_2$, Solid State Ionics 86–88 (1995) 791.
[41] R.D. Shannon, C.T. Prewitt, Synthesis and properties of $LiNiO_2$ as cathode material for secondary batteries, Acta Crystallogr. B25 (1969) 925.
[42] Y. Uchimoto, H. Sawada, Changes in electronic structure by Li ion intercalation in $LiNiO_2$ from nickel L-edge XANES, J. Power Sources 97 ($_{2001}$) 326.
[43] M.K. Aydinol, A.F. Kohan, G. Cedar, Ab initio calculation of the intercalation voltage of lithium transition metal oxide electrodes for rechargeable batteries, J. Power Sources 68 (1997) 664.
[44] R.V. Moshtev, P. Zlatilova, V. Manev, A. Sato, The $LiNiO_2$ solid solution as a cathode material for rechargeable lithium batteries, J. Power Sources 54 (2) (1995) 329.
[45] W. Li, J.N. Reimers, J.R. Dahn, In situ X-ray diffraction and electrochemical studies of $Li_{1-x}NiO_2$, Solid State Ionics 67 (1–2) (1993) 123.
[46] A.T. Hewston, B.L. Chamberland, A survey of first-row ternary oxides $LiMO_2$ (M = Sc–Cu), J. Phys. Chem. Solids 48 (1987) 97.
[47] R. Koksbang, J. Barker, H. Shi, M.Y. Saïdi, Cathode materials for lithium rocking chair batteries, Solid State Ionics 84 (1–2) (1996).
[48] J.R. Dahn, E.W. Fuller, M. Obrovac, U. von Sacken, Thermal and electrochemical properties of of Li_xCoO_2 and Li_xNiO_2, Phys. Rev. B46 (1992) 3236.

[49] N. Imanishi, M. Fujii, A. Hirano, Y. Takeda, M. Inaba, Z. Ogumi, Structure and electrochemical behaviors of Li_xCoO_2 treated under high oxygen pressure, Solid State Ionics 140 (2001) 45.

[50] J.B. Goodenough, D.G. Wickham, Some magnetic and crystallographic properties of the system $Li_x^+Ni_{1-2x}^{++}Ni_x^{+++}O$, J. Phys. Chem. Solids 5 (1958) 107.

[51] A. Rougier, C. Delmas, G. Chouteau, Magnetism of $Li_{1-z}Ni_{1+z}O_2$: A powerful tool for structure determination, J. Phys. Chem. Solids 57 (1996) 1101.

[52] M. Kitaoka, Y. Iwakoshi, H. Komori, Comparative study of $LiCoO_2$, $LiNi_{1/2}Co_{1/2}O_2$ and $LiNiO_2$ for 4 volt secondary lithium cells, Electrochim. Acta 38 (9) (1993) 1159.

[53] J.R. Dahn, E.W. Fuller, M. Obrovac, U. von Sacken, Thermal stability of Li_xCoO_2, Li_xNiO_2 and λ-MnO_2 and consequences for the safety of Li-ion cells, Solid State Ionics 69 (1994) 265.

[54] H. Arai, S. Okada, Y. Sakurai, J. Yamaki, Thermal behavior of $Li_{1-y}NiO_2$ and the decomposition mechanism, Solid State Ionics 109 (1998) 295.

[55] X.Q. Yang, X. Sun, J. McBreen, Structural changes and thermal stability: in situ X-ray diffraction studies of a new cathode material $LiMg_{0.125}Ti_{0.125}Ni_{0.75}O_2$, Electrochem. Commun. 2 (10) (2000) 733.

[56] M.G.S.R. Thomas, W.I.F. David, J.B. Goodenough, J. Molenda, P. Wilk, J. Marzec, Structural, electrical and electrochemical properties of $LiNiO_2$, Mater. Res. Bull. 20 (1985) 1137.

[57] R. Kanno, H. Kubo, Y. Kawamoto, T. Kamiyama, F. Izumi, Y. Takeda, M. Takano, Phase relationship and lithium deintercalation in lithium nickel oxides, J. Solid State Chem. 110 (1994) 216.

[58] D. Larcher, M.R. Palacin, A. Andemer, N. Sac-Epée, G.G. Amatucci, J.M. Tarascon, Electrochemical performances of layered $LiM_{1-y}My'O_2$ (M=Ni, Co; M′=Mg, Al, B) oxides in lithium batteries, Solid State Ionics 135 (1–4) (2000) 121.

[59] A. Rougier, C. Delmas, A.V. Chadwick, Non-cooperative Jahn-Teller effect in $LiNiO_2$: an EXAFS study, Solid State Commun. 94 (1995) 123.

[60] I. Nakai, K. Takahashi, Y. Shiraishi, T. Nakagome, F. Nishikawa, Study of the Jahn-Teller distortion in $LiNiO_2$, a cathode material in a rechargeable lithium battery, by in situ X-ray absorption fine structure analysis, J. Solid State Chem. 140 (1998) 145.

[61] K. Suzuki, Y. Kuroiwa, S. Takami, M. Kubo, M. Miyamoto, Combinatorial computational chemistry approach to the design of cathode materials for a lithium secondary battery, Appl. Surf. Sci. 189, 3–4, 28 (2002).

[62] G. Prado, L. Fournes, C. Delmas, The $Li_xNi_{0.70}Fe_{0.15}Co_{0.15}O_2$ system: an X-ray diffraction and Mössbauer study, J. Solid State Chem. 159 (2001) 103.

[63] J.P. Peres, C. Delmas, A. Rougier, M. Broussely, F. Perton, P. Biensan, P. Willmann, The relationship between the composition of lithium nickel oxide and the loss of reversibility during the first cycle, J. Phys. Chem. Solids 57 (1996) 1057.

[64] T. Ohzuku, H. Konori, M. Nagayama, K. Sawai, Synthesis and electrochemical characteristics of $Li(NiM)O_2$ (M= Co, Mn) cathode for rechargeable lithium batteries, J. Power Sources 68 (2) (1997) 545.

[65] W. Li, J.N. Reimers, J.R. Dahn, Synthesis and electrochemical properties for $LiNiO_2$ substituted by other elements, Solid State Ionics 67 (1993) 123.

[66] Z. Lu, X. Huang, H. Huang, L. Chen, J. Schooman, Synthesis and properties of gallium-doped $LiNiO_2$ as the cathode material for lithium secondary batteries, Solid State Ionics 120 (1999) 103.

[67] M. Broussely, F. Perton, J. Labat, R.J. Staniewicz, A. Romero, Li/Li_xNiO_2 and Li/Li_xCoO_2 rechargeable systems: comparative study and performance of practical cells, J. Power Sources 43-44 (1993) 209.

[68] K. Kubo, M. Fujiwara, S. Yamada, S. Arai, M. Kanda, Synthesis and electrochemical properties for bi-substituted $LiNiO_2$, J. Power Sources 68 (2) (1997) 533.

[69] S. Yamada, M. Fujiwara, M. Kanda, On the electrochemical properties of $LiNiO_2$ as cathode material for secondary batteries, J. Power Sources 34 (1994) 209.

[70] T. Ohzuku, A. Ueda, M. Nagayama, Crystal structures and electrochemical properties of $LiAl_yNi_{1-y}O_2$ solid solution, J. Electrochem. Soc. 140 (1993) 1962.

[71] T. Ozhuku, H. Konori, M. Nagayama, K. Sawai, T. Hirai, Lithium-ion battery for electronic applications, Chem. Exp. 6 (1991) 161.

[72] W. Li, J.N. Reimers, J.R. Dahn, Storage characteristics of cathodes for Li-ion batteries, Solid State Ionics 67 (1993) 123.

[73] Z. Lu, X. Huang, H. Huang, L. Chen, J. Schooman, Reversibility of $LiNiO_2$ cathode, Solid State Ionics 120 (1999) 103.

[74] M. Broussely, F. Perton, J. Labat, R.J. Staniewicz, Influence of morphology on the stability of $LiNiO_2$, J. Power Sources 43–44 (1993) 209.

[75] M. Mohan Rao, M. Jayalakshmi, O. Schaff, U. Guth, H. Wulff, F. Scholz, Electrochemical behavior of solid lithium nickelate ($LiNiO_2$) in aqueous electrolyte system, J. Solid State Electrochem. 4 (1999) 17.

[76] T. Ohzuku, H. Komori, K. Sawai, T. Hirai, Electrochemical performance and chemical properties of oxidic cathode materials for 4V rechargeable Li-ion batteries, Chem. Exp. 5 (1990) 733.

[77] C. Pouillerie, L. Croguennec, C. Delmas, The $Li_xNi_{1-y}Mg_yO_2$ (y= 0.05, 0.10) system: structural modifications observed upon cycling, Solid State Ionics 132 (2000) 15.

[78] J. Kim, K. Amine, The effect of tetravalent titanium substitution in $LiNi_{1-x}Ti_xO_2$ ($0.025 \leq x \leq 0.2$) system, Electrochem. Commun. 3 (2001) 52.

[79] M. Spahr, P. Nivak, B. Schnyder, O. Haas, R. Nespar, Characterization of layered lithium nickel manganese oxide synthesized by a novel oxidative co-precipitation method and their electrochemical performance as lithium insertion electrode material, J. Electrochem. Soc. 145 (1998) 1113.

[80] C. Delmas, G. Prado, A. Rougier, E. Suard, L. Fournès, Effect of iron on the electrochemical behaviour of lithium nickelate from $LiNiO_2$ to 2D-$LiFeO_2$, Solid State Ionics 135 (2000) 71.

[81] Z.Q. Yang, X. Sun, J. Mc Breen, Structural changes and thermal stability: in situ X-ray diffraction studies of a new cathode material $LiMg_{0.125}Ti_{0.125}Ni_{0.75}O_2$, Electrochem. Commun. 2 (2000) 733.

[82] K.K. Lee, K.B. Kim, Structural chemistry of $LiNiO_2$ for 4V secondary lithium cells, J. Electrochem. Soc. 147 (2000) 1709.

[83] Y. Cho, Y.J. Kim, B. Park, New findings on the phase transitions in $Li_{1-x}NiO_2$: in in situ synchrotron X-ray diffraction studies, Chem. Mater. 12 (2003) 3788.

[84] Y. Cho, G.B. Kim, H.S. Lim, C.S. Kim, S.Y. Yoo, Improvement of structural stability of $LiMn_2O_4$ cathode materials on 55 °C cycling by sol–gel coating of $LiCoO_2$, Electrochem. Soild State Lett. 2 (1999) 607.

[85] Y. Cho, G.B. Kim, H.S. Lim, C.S. Kim, S.Y. Yoo, High-performance ZrO_2 coated $LiNiO_2$ cathode materials, Electrochem. Soild State Lett. 4 (2001) 159.

[86] B.V.R. Chowdari, G.V. Subbarao, S.Y. Chow, The effects of sintering temperature and time on the structure and electrochemical performance of $LiNi_{0.8}Co_{0.2}O_2$ cathode materials derived from sol–gel method, J. Solid State Electrochem. 7 (2003) 456.

[87] H. Liu, Z. Zhang, Z. Gong, Y. Yang, A comparative study of $LiNi_{0.8}Co_{0.2}O_2$ cathode materials modified by lattice-doping and surface-coating, Solid State Ionics 166 (2004) 317.